Direct patterning of solution-processed organic thin-film transistor by selective control of solution wettability of polymer gate dielectric

Yoshihide Fujisaki, Hiroshi Ito, Yoshiki Nakajima, Mitsuru Nakata, Hiroshi Tsuji, Toshihiro Yamamoto, Hirokazu Furue, Taiichiro Kurita, and Naoki Shimidzu

Citation: Applied Physics Letters **102**, 153305 (2013); doi: 10.1063/1.4802499
View online: http://dx.doi.org/10.1063/1.4802499
View Table of Contents: http://scitation.aip.org/content/aip/journal/apl/102/15?ver=pdfcov
Published by the AIP Publishing

Direct patterning of solution-processed organic thin-film transistor by selective control of solution wettability of polymer gate dielectric

Yoshihide Fujisaki,[1] Hiroshi Ito,[2] Yoshiki Nakajima,[1] Mitsuru Nakata,[1] Hiroshi Tsuji,[1] Toshihiro Yamamoto,[1] Hirokazu Furue,[2] Taiichiro Kurita,[1] and Naoki Shimidzu[1]
[1]*NHK Science and Technology Research Laboratories, Kinuta, Setagaya-ku, Tokyo 157–8510, Japan*
[2]*Department of Materials Sciences and Technology, Tokyo University of Science, Yamazaki, Noda-Shi, Chiba 278–8510, Japan*

(Received 21 January 2013; accepted 7 April 2013; published online 18 April 2013)

A simple direct patterning method for solution-processable organic semiconductors (OSCs) is demonstrated. The solution-wettable and nonwettable regions of a polymer gate dielectric layer were selectively controlled by a short tetrafluoromethane gas plasma treatment, and we precisely patterned the OSC film in the desired channel region by lamination coating. The patterned OSC films represent polycrystalline structures consisting of crystalline domains varying from 30 to 60 μm, and the resulting short-channel thin-film transistor (TFT) showed a high mobility of up to 1.3 cm^2/Vs, a large on/off ratio over 10^8, and a negligible hysteresis curve. The proposed method is scalable for patterning TFT arrays with large-area dimensions. © *2013 AIP Publishing LLC* [http://dx.doi.org/10.1063/1.4802499]

Solution-processable organic thin-film transistors (OTFTs) are attracting considerable attention owing to both their simple and facile manufacturing processes and excellent transistor performance.[1] To date, many efforts have been made focusing on the deposition of a solution-processable organic semiconductor (OSC) film by various approaches, such as spin coating, drop casting, and ink-jet printing.[2–4] In recent years, several studies have demonstrated devices based on single-crystal or highly crystalline thin films with high mobilities exceeding 5 cm^2/Vs.[5–8] The obtained results open a new window for a wide range of applications, such as integrated circuits and sensors and high-resolution and large-area flexible displays. In many cases, however, a discrete device or a top-contact configuration with a longer channel length is often used. Considering commercial applications, the development of short channel thin-film transistors (TFTs) is a key issue for increasing the output current and operating frequency. However, with only a few exceptions reported, such as ink-jet printing,[9] dry taping approach,[10] and poly (dimethylsiloxane) stamp,[11] there have been only a few reports regarding high mobility solution-processable OTFTs with practical device dimensions. To achieve such short-channel devices, the OSC film should be precisely patterned to reduce parasitic current paths from one device to another device and obtain a higher current on/off ratio. For solution-processable OTFTs, therefore, it is still a challenge to develop a precise and high-resolution pattern of the OSC film by a simple solution process.

The selective control of the solution wettability of the gate dielectric is one of the attractive ways to form a confined pattern of the OSC film. Recently, self-assembled monolayers (SAMs) with different functionalities have been utilized to create selective wettability on the surface of the gate dielectric.[12–14] However, the reproducibility and uniform coverage of the SAM layer are still technical challenges for the practical application. The long processing time for the reaction of SAM treatments is also an obstacle to the industrial application. Furthermore, when low-cost and solution processes are considered, the direct control of the surface of the solution-processable polymer dielectric is more desirable.

In this article, we present a simple direct patterning method for solution-processable OSC for developing a high-mobility short-channel TFT array. The solution-wettable and nonwettable regions of a cross-linkable olefin-type polymer dielectric layer were created by the selective exposure of tetrafluoromethane (CF_4) gas plasma. A soluble small-molecule OSC was precisely patterned by drop casting and lamination coating. The key advantages of this proposed method are the clear shape of the patterned film, the small consumption of the OSC droplet, and the utilization of the inherent interface conditions of polymer gate dielectric. By this simple method, the OSC film was directly patterned in the confined active channel region.

All the fabrication processes and measurements were performed under ambient air conditions. The fabrication and patterning processes are schematically shown in Fig. 1. A bottom-contact TFT array was fabricated on a glass or plastic film that was bonded onto a support glass. The choice of polymer gate dielectric material is very important, because the surface or interface condition of the dielectric layer affects the wettability and spreading of the OSC solution in addition to the molecular alignment and crystalline nature. The dielectric constant, chemical structure, and functional group of the dielectric material affect the electrical characteristics, such as mobility, hysteresis, and subthreshold slope (SS).[15–17] In this study, we employed a cross-linkable olefin-type polymer with a moderate hydrophobicity, a low dielectric constant of 2.7 (at 1 kHz), and a surface structure without polar functionalities, such as the hydroxyl group.[18,19] This polymer was dissolved in 20 wt. % diethylene glycol ethyl methyl ether (EDM) and thermally cross-linked by 150 °C cure treatment. A schematic illustration of this polymer structure is shown in Fig. 1(a). For the OSC material, we used a mesitylene-based formulation of a soluble small-molecule OSC (lisicon®1200 Merck Chemicals Ltd.)[20] with

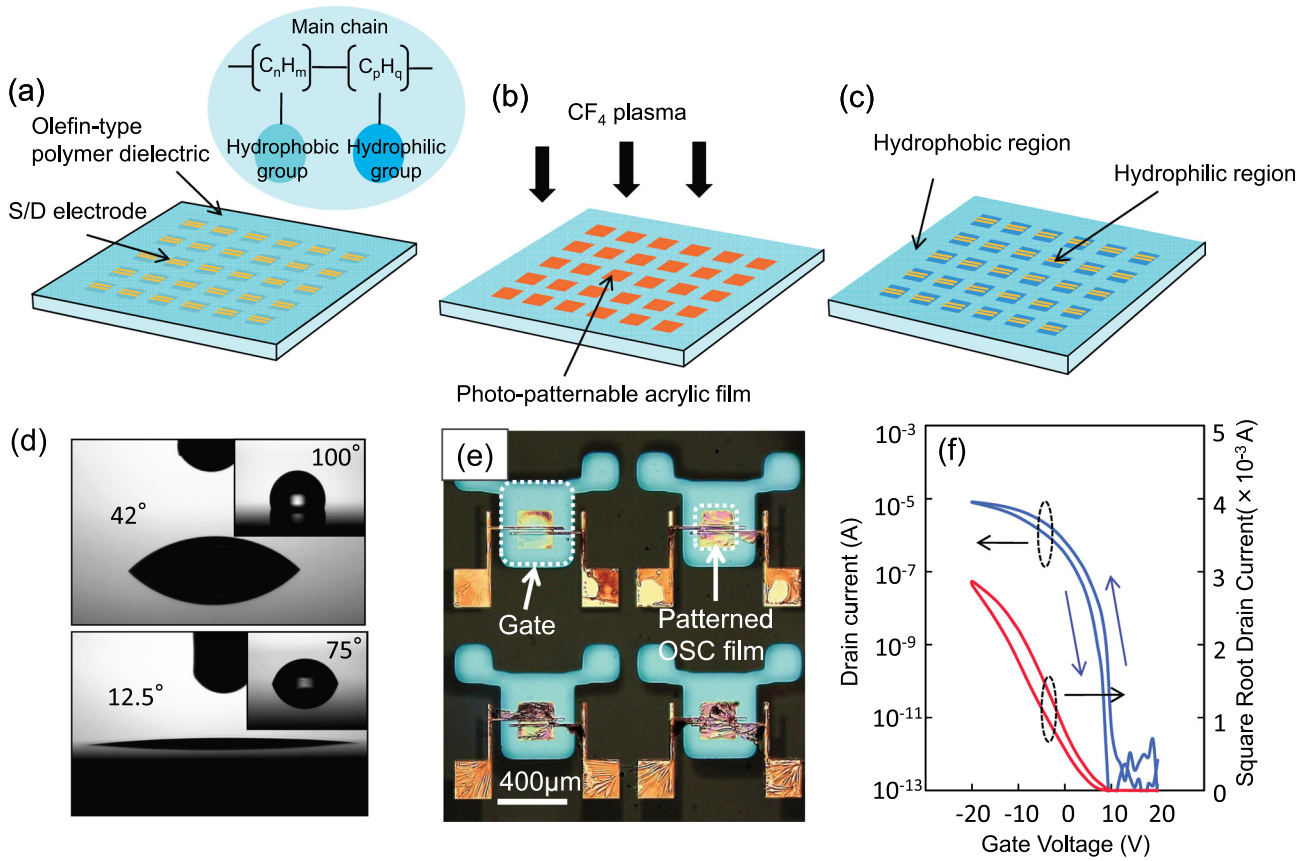

FIG. 1. (a)-(c) Schematic illustration of fabrication and patterning processes for OTFT array. After patterning the S/D electrode, the entire surface was modified using CF_4 plasma except the channel region. (d) Mesitylene contact angles of CF4 plasma-treated non-channel (upper) and channel regions (lower). Insets show water contact angles. (e) Optical microscopy image of TFT array structure with patterned OSC film. (f) Transfer characteristics of fabricated bottom-contact TFT with channel length L = 10 μm.

a deep ionization potential (IP) of 5.4 eV in order to induce a slow solvent evaporation. After the patterning of the gate electrode of Mo, a 300-nm-thick olefin-type polymer dielectric layer was formed by spin coating followed by curing at 150 °C on a hot plate. Au source/drain (S/D) electrode was then deposited and patterned by wet etching followed by surface modification using a thiol-based SAM (Fig. 1(a)).[21] The template for the patterning of the OSC film was fabricated as follows. First, the surface of the polymer dielectric layer of the active channel region, which is located inside the gate electrode region, was covered with a conventional photo patternable acrylic film. Then, the entire surface of the substrate was exposed to radio-frequency (RF) tetrafluoromethane (CF_4) gas plasma for a short time (Fig. 1(b)). The CF_4 plasma treatment resulted in a hydrophobic surface owing to a highly fluorinated surface.[22,23] However, excess plasma treatments induce surface roughening or undesirable surface unevenness with the etching of the polymer layer; thus, we investigated the minimum plasma conditions for the saturation of surface modification by varying the RF power ranging from 30 to 300 W and exposure time. From the results, we found that plasma treatment for 10 s with an RF power of 100 W is adequate for obtaining a reproducible hydrophobic surface while minimally affecting the surface roughness. After the removal of the cover film, the contact angle (CA) of the plasma-treated surface region was increased except in the channel region with an inherent polymer nature with a relatively hydrophilic surface (Fig. 1(c)). Figure 1(d) shows the mesitylene and water contact angle of the plasma-treated non-channel and untreated channel regions.

To confirm the patterning ability of the fabricated template, we first drop-casted a small amount of OSC solution on the template. To prevent the formation of a thick or aggregated film, a relatively low concentration (0.08 wt. %) of mesitylene solution was dropped and dried on a hot plate heated at 50 °C for 1 h in air. As shown in Fig. 1(d), we obtained a clear contact angle difference of approximately 30°; therefore, the patterning of the OSC layer was self-organized within the channel region (nonfluorinated region). Figure 1(e) shows the optical microscopy image of the fabricated bottom-contact TFT array. Figure 1(f) shows the transfer characteristics of the fabricated short-channel TFT with a channel length L of 10 μm. Although, as shown in the figure, the fabricated TFT showed a low off-current below 10^{-12} A, large saturation mobility variations ranging from 0.1 to 0.5 cm^2/Vs were observed. This is possibility due to the poor reproducibility of film thickness and insufficient crystallinity, as shown in Fig. 1(e).

As the next step, in order to improve the TFT performance, we patterned the OSC film by a method combining drop casting and lamination coating based on the recently reported solution shearing[24] and push coating methods.[25] A schematic illustration of this method is shown in Fig. 2(a). After a drop cast of 20 μl of OSC solution, the OSC droplet was squashed by the lamination of an upper plastic film (100-μm-thick poly (ethylene naphthalate) film was used in this study). To obtain a strong de-wettable surface against

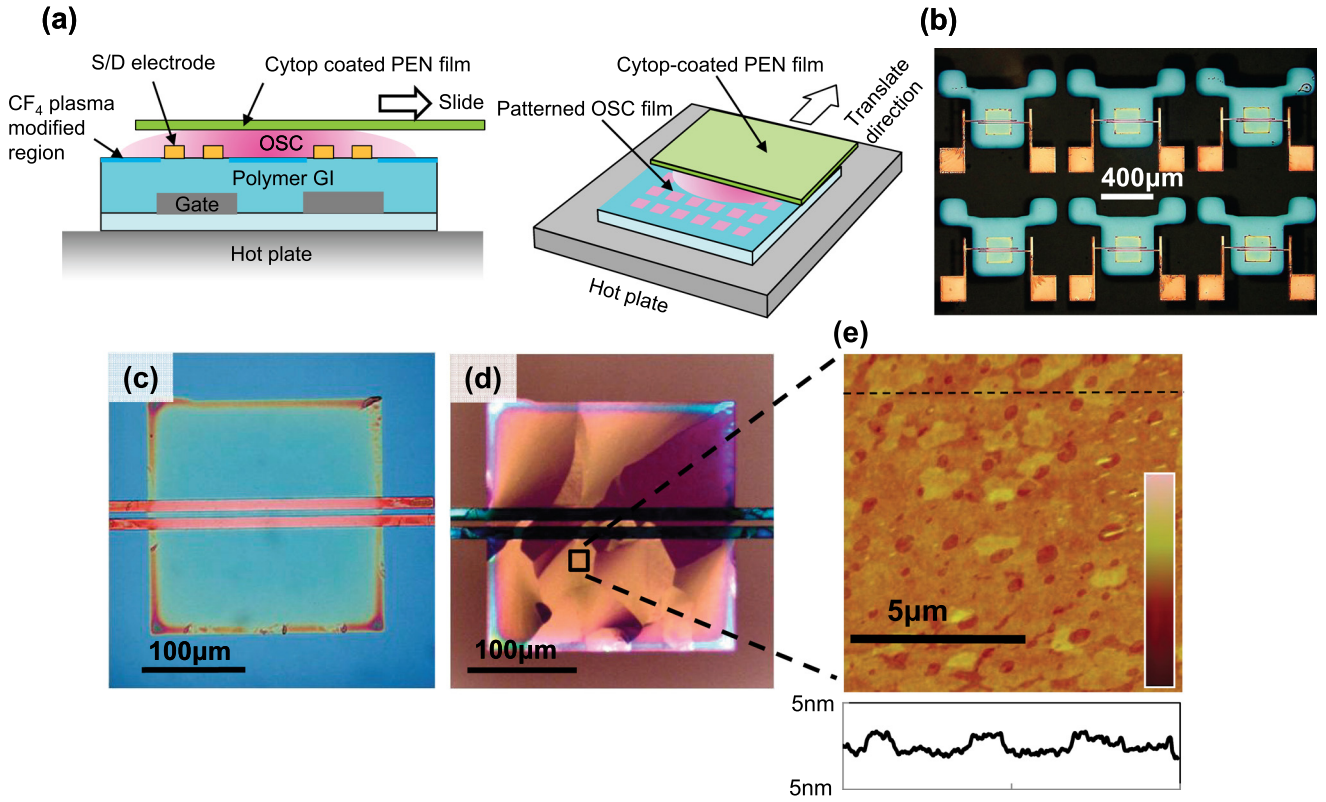

FIG. 2. (a) Schematic illustration of lamination coating and patterning of OSC film. (b) Optical microscopy image of TFT array structure with precisely patterned OSC film and (c) magnified image of OSC film within active channel region. (d) Cross-polarized microscopy image of patterned OSC film and (e) AFM topography image of local film shown in Fig. 3(d). The height scale is 20 nm.

the OSC droplet, the contact side of the film was in advance with the fluoro polymer Cytop™ (Asahi Glass, Japan). The CA of mesitylene for the Cytop-coated film was approximately 51°, which is slightly higher than that in the CF_4 plasma-treated region. The OSC droplet was uniformly spread on the entire surface of the gate dielectric layer owing to the de-wettability of the film. Then, the device was transferred onto a hot plate heated from 30 to 100 °C. The top film was then translated slowly at a constant speed. The OSC solution gradually exposed to air was rapidly gathered in a hydrophilic active channel region during the slow evaporation of the solvent. Consequently, we crystallized the OSC film precisely in the active channel region.

Figure 2(b) shows the optical microscopy image of the OTFT array structure fabricated by this method. In this case, 1 wt. % OSC solution was drop-casted, and the upper substrate was translated at a substrate temperature of 50 °C. The OSC film was precisely patterned and crystallized within the 200 μm^2 channel region (Fig. 2(c)). The cross-polarized optical microscopy image of the patterned OSC film is also shown in Fig. 2(d). The clear birefringence indicates that relatively large well-ordered polycrystalline domains, which vary from approximately 30 to 60 μm, were formed within the prescribed channel region. To further investigate the structure of the patterned OSC film, we examined the surface morphology of the film by tapping-mode AFM. Figure 2(e) exhibits the topography and cross-sectional height image of a local OSC film near the S/D contact shown in Fig. 2(d). The OSC film exhibited a smooth terrace and step morphology except at the boundary of crystalline domains. The step height was estimated to be approximately 2 nm from the cross section. However, the planar at the molecular level was not very large, and we observed nanoscale elliptically shaped holes, which may be generated by the evaporation or bumping of the residual solvent in the OSC film. These results indicate that evaporation speed is still high; thus, we consider that further optimization will be required to obtain a uniform and continuous film.

Figures 3(a) and 3(b) exhibit the typical transfer and output curves of the fabricated short-channel TFT with $L = 5\ \mu$m, respectively. As shown in these figures, complete isolation of the OSC layer from the neighboring devices resulted in a very low off-current of 10^{-13} A and a very high on/off ratio of more than 10^8. To extract characteristic parameters from DC electrical measurements under ambient air, it is important to minimize the effect of moisture-induced surface polarization or ion diffusion effect;[26] thereby, low-frequency capacitance-voltage characteristics were used to estimate the gate capacitance C_G (17.7 nFcm^{-2} at 20 Hz). The device showed a high mobility of up to 1.3 cm^2/Vs. A low SS of 0.39 V/dec and a negligible small hysteresis curve indicate that trap states, which often originate from polar groups at the surface of the insulator,[27,28] are few. The maximum trap density was calculated to be 5.6×10^{11} cm^{-2} eV^{-1} according to[29]

$$N_{trap}^{max} \approx \left[\frac{qS\log(e)}{kT} - 1\right]\frac{C_{OX}}{q},$$

where q is the electronic charge, S is the SS, k is Boltzmann's constant, and C_{OX} is the gate capacitance (per unit of area). We consider that these results are attributed to the utilization of the inherent surface property of the polymer dielectric.

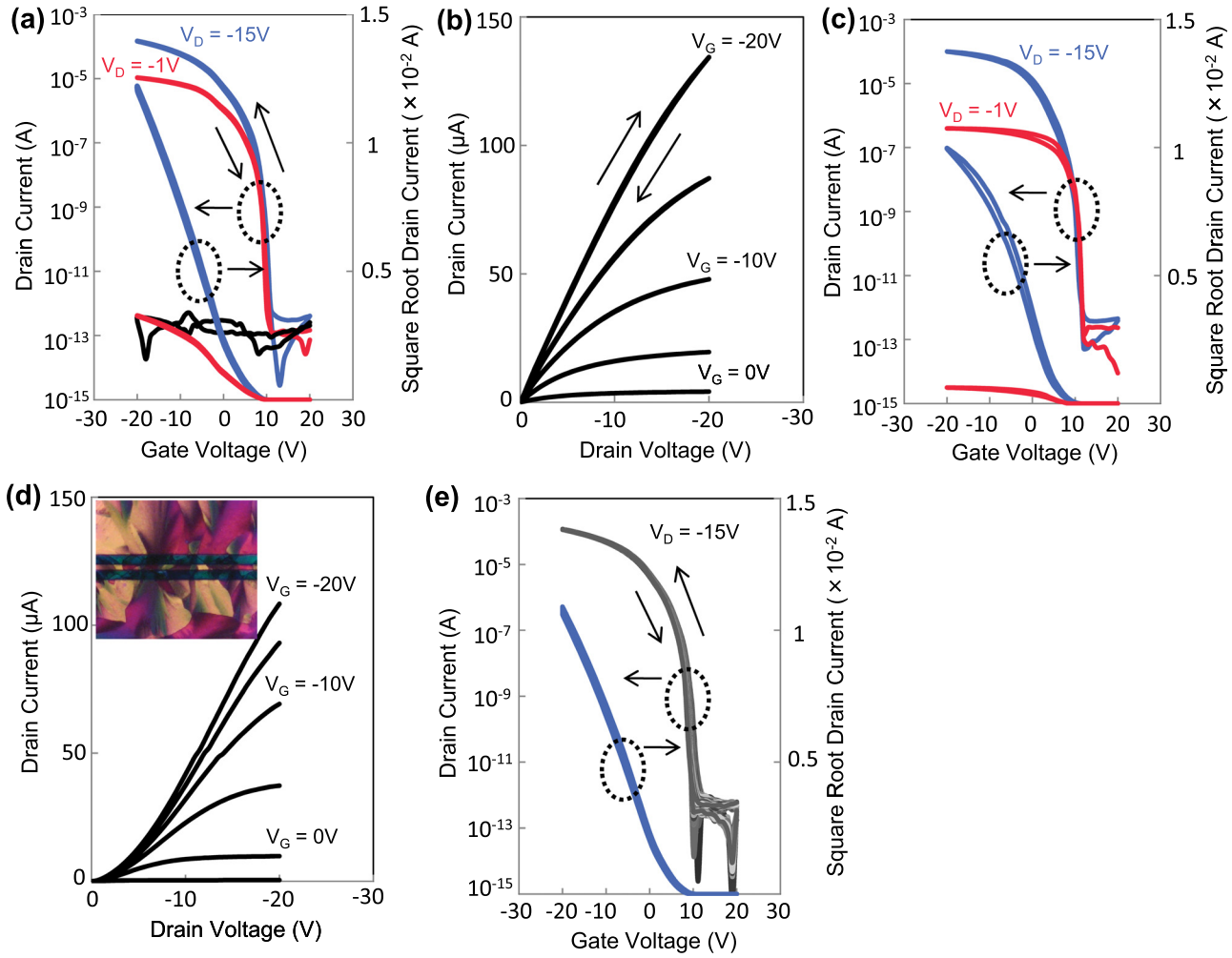

FIG. 3. (a) Transfer and (b) output characteristics of bottom-contact OTFTs. The channel length (L) and width (W) are 5 and 200 μm, respectively. (c) Transfer and (d) output characteristics of another device with large contact resistance and inset shows the corresponding cross-polarized microscopy image of the OSC film. (e) Results of repeated 100 cycle test under ambient air.

The fabricated array showed characteristic variations. Figures 3(c) and 3(d) show the TFT performance of another device in the same array. The transfer and output curves exhibited an injection-limited curve at a low drain voltage owing to a large contact resistance (R_C). To investigate the cause of the large R_C, the energy level mismatch between the Fermi-level of the SAM-treated Au contacts and the HOMO of the OSC film was measured by photoelectron yield spectroscopy (Riken Keiki, AC-3). The energetic difference was found to be not very large at 0.06 eV, which is comparable to those of Au and pentacene; thus, we considered that the large R_C is mainly caused by the formation of defects due to the disordered or misalignment crystalline structure near the S/D contact.[30,31] Actually, we observed randomly polarized small domain near the contacts in the large R_C device, as shown in the inset in Fig. 3(d). We speculate that this is due to the rough edge structure of the bottom S/D contacts or the local differential of the solvent wettability between Au and the polymer dielectric; thus, the optimization of the contact structure and surface modification will contribute to further improvements in the characteristics. As discussed in Fig. 2(e), a slower solvent evaporation will also help create highly crystalline films with fewer defects. Finally, in order to evaluate simply the air-stability of the fabricated TFT, a cycling test was performed under ambient air conditions. As shown in Fig. 3(e), the fabricated device exhibited very little degradation in mobility and on/off ratio after repeated 100 cycles. We consider that this is due to the deep IP of the OSC film and the low interface trap density of polymer gate dielectric.

In summary, we have demonstrated a short-channel bottom-contact OTFT array with a finely patterned OSC film. The solvent wettability of the polymer gate dielectric was controlled by the selective exposure of CF_4 plasma, and the solution-processed OSC film was directly patterned and crystallized within the channel region by the lamination coating. The fabricated short-channel TFT showed a high mobility of up to 1.3 cm^2/Vs and a very large on/off ration over 10^8. These techniques are scalable for patterning high-resolution OTFT arrays with large-area dimensions.

The authors thank Zeon Co., Ltd. for providing the polymer dielectric material and for various discussions.

[1]*Organic Field-Effect Transistors*, edited by Z. Bao and J. Locklin (CRC, Boca Raton, FL, 2007).
[2]D. J. Gundlach, J. E. Royer, S. K. Park, S. Subramanian, O. D. Jurchescu, B. H. Hamadani, A. J. Moad, R. J. Kline, L. C. Teague, O. Kirillov, C. A. Richter, J. G. Kushmerick, L. J. Richter, S. R. Perkin, T. N. Jackson, and J. E. Anthony, Nature Mater. **7**, 216 (2008).

[3]S. K. Park, J. E. Anthony, and T. N. Jackson, IEEE Electron Device Lett. **28**, 877 (2007).
[4]A. C. Arias, J. Daniel, S. Sambandan, T. N. Ng, B. Russo, B. Krusor, and R. A. Street, Proc. SPIE **7054**, 70540L-1 (2008).
[5]H. Minemawari, T. Yamada, H. Matsui, J. Tsutsumi, S. Haas, R. Chiba, R. Kumai, and T. Hasegawa, Nature (London) **475**, 364 (2011).
[6]J. Soeda, Y. Hirose, M. Yamagishi, A. Nakao, T. Uemura, K. Nakayama, M. Uno, Y. Nakazawa, K. Takimiya, and J. Takeya, Adv. Mater. **23**, 3309 (2011).
[7]H. Li, B. C. Tee, J. J. Cha, Y. Cui, J. W. Chung, S. Y. Lee, and Z. Bao, J. Am. Chem. Soc. **134**, 2760 (2012).
[8]J. Smith, W. Zhang, R. Sougrat, K. Zhao, R. Li, D. Cha, A. Amassian, M. Heeney, I. McCulloch, and T. Anthopoulos, Adv. Mater. **24**, 2441 (2012).
[9]T. N. Ng, S. Sambandan, R. Lujan, A. C. Arias, C. R. Newman, H. Yan, and A. Facchetti, Appl. Phys. Lett. **94**, 233307 (2009).
[10]S. Liu, H. A. Becerril, M. C. LeMieux, W. M. Wang, J. H. Oh, and Z. Bao, Adv. Mater. **21**, 1266 (2009).
[11]K. C. Dickey, S. Subramanian, J. E. Anthony, L. H. Han, S. Chen, and Y. L. Loo, Appl. Phys. Lett. **90**, 244103 (2007).
[12]T. Minari, M. Kano, T. Miyadera, S.-D. Wang, Y. Aoyagi, M. Seto, T. Nemoto, S. Isoda, and K. Tsukagoshi, Appl. Phys. Lett. **92**, 173301 (2008).
[13]M. Kano, T. Minari, and K. Tsukagoshi, Appl. Phys. Express **3**, 051601 (2010).
[14]W. Kang, M. Kitamura, and Y. Arakawa, Appl. Phys. Express **4**, 121602 (2011).
[15]J. Veres, S. Ogier, G. Lloyd, and D. de Leeuw, Chem. Mater. **16**, 4543 (2004).
[16]J. Jang, S. Nam, D. S. Chung, S. H. Kim, W. M. Yun, and C. E. Park, Adv. Funct. Mater. **20**, 2611 (2010).
[17]J. Li, J. Du, J. Xu, H. L. W. Chan, and F. Yan, Appl. Phys. Lett. **100**, 033301 (2012).
[18]Y. Isogai, T. Katoh, K. Sugitani, M. Hanmura, M. Tada, Y. Nakajima, Y. Fujisaki, and T. Yamamoto, SID Symp. Dig. **42**, 1581 (2011).
[19]Y. Fujisaki, T. Kono, Y. Nakajima, T. Takei, J. Nishida, T. Yamamoto, and Y. Yamashita, Appl. Phys. Lett. **97**, 133303 (2010).
[20]G. Lloyd, T. Backlund, P. Brookes, L. W. Tan, P. Wierzchowiec, J.-Y. Lee, S. Bain, M. James, J. Canisius, S. Tierney, K. Kawamata, and T. Wakimoto, Proc. IDW **10**, 469 (2010).
[21]Y. Fujisaki, Y. Nakajima, T. Takei, H. Fukagawa, T. Yamamoto, and H. Fujikake, IEEE Trans. Electron Devices **59**, 3442 (2012).
[22]Y. H. Yan, M. B. Park, and C. Y. Yue, Langmuir **21**, 8905 (2005).
[23]C. S. Kim, S. J. Jo, J. B. Kim, S. Y. Ryu, J. H. Noh, H. K. Baikb, S. J. Lee, and Y. S. Kim, Appl. Phys. Lett. **91**, 063503 (2007).
[24]Z. Liu, H. A. Becerril, M. E. Roberts, Y. Nishi, and Z. Bao, IEEE Trans. Electron Devices **56**, 176 (2009).
[25]M. Ikawa, T. Yamada, H. Matsui, H. Minemawari, J. Tsutsumi, Y. Horii, M. Chikamatsu, R. Azumi, R. Kumai, and T. Hasegawa, Nat. Commun. **3**, 1176 (2012).
[26]T. Jung, A. Dodabalapur, R. Wenz, and S. Mohapatra, Appl. Phys. Lett. **87**, 182109 (2005).
[27]S. Lee, B. Koo, J. Shin, E. Lee, and H. Park, Appl. Phys. Lett. **88**, 162109 (2006).
[28]N. B. Ukah, J. Granstrom, R. R. S. Gari, G. M. King, and S. Guha, Appl. Phys. Lett. **99**, 243302 (2011).
[29]M. McDowell, I. G. Hill, J. E. McDermott, S. L. Bernasek, and J. Schwartz, Appl. Phys. Lett. **88**, 073505 (2006).
[30]S. D. Wang, T. Miyadera, T. Minari, Y. Aoyagi, and K. Tsukagoshi, Appl. Phys. Lett. **93**, 043331 (2008).
[31]K.-D. Jung, Y. C. Kim, H. Shin, B.-G. Park, J. D. Lee, E. S. Cho, and S. J. Kwon, Appl. Phys. Lett. **96**, 103305 (2010).